



An assessment of metal bioremoval potential of *Chlorella minutissima* from synthetic industrial effluents

Shailendra Kumar Singh¹, Ajay Bansal², M. K. Jha², Gerard Abraham³, Rupak Kumar^{4*}

Received: 15 February 2023 / Accepted: 14 July 2023 / Published: 30 September 2023

¹Department of Biochemistry, S.S. Khanna Girls Degree College, Prayagraj, India.

²Department of Chemical Engineering, Dr. B. R. Ambedkar National Institute of Technology, Jalandhar, India.

³Indian Agricultural Research Institute (ICAR), New Delhi, India.

⁴Indian Council of Medical Research (ICMR), New Delhi, India.

*Correspondence

Rupak Kumar

rupakraman@gmail.com

Microalgae offer a sustainable approach for removing heavy metals from industrial effluents. This study evaluated the ability of *Chlorella minutissima* to tolerate and remove Cd²⁺, Cr⁶⁺, Pb²⁺, and Zn²⁺ from synthetic wastewater under optimized growth conditions (27 ± 1 °C, pH 7.5, 14:10 h light: dark cycle, 2000–2500 lux, 100 mgL⁻¹ glucose, initial density ≥10⁶ cells mL⁻¹). Growth responses and metal uptake were assessed across concentrations of 0.5–10 mgL⁻¹. Results showed strong variability among metals. At 0.5 mgL⁻¹, the highest removal percentage was recorded for Zn²⁺ (98.63%), followed by Pb²⁺ (93.15%), Cr⁶⁺ (85.69%), and Cd²⁺ (40.49%). However, Pb²⁺ exhibited the highest absolute uptake amount (6.86 µg per 100 mL) at 3 mgL⁻¹, while Cr⁶⁺ underwent significant intracellular reduction to Cr³⁺. Growth inhibition was most pronounced under Cd²⁺ exposure, followed by Cr⁶⁺, Pb²⁺, and Zn²⁺. Negative controls confirmed normal growth in the absence of metals. These findings indicate that *C. minutissima* is an effective biosorbent for low concentrations of Pb²⁺, Zn²⁺, and Cr⁶⁺ under laboratory conditions. While the results highlight its potential for wastewater treatment, further studies using real effluents and pilot-scale systems are necessary to establish practical applicability.

Keywords: *Chlorella minutissima*, heavy metals, bioremoval, bioadsorption, bioabsorption, bioreduction, wastewater treatment

Introduction

The rapid pace of industrialization worldwide has led to a significant increase in the discharge of untreated effluents containing heavy metals such as lead (Pb²⁺), chromium (Cr⁶⁺), cadmium (Cd²⁺), copper (Cu²⁺), nickel (Ni²⁺), and zinc (Zn²⁺). Conventional metal removal technologies including chemical precipitation, oxidation–reduction, ion exchange, electrolysis, and membrane filtration have been widely employed. However, these methods are often ineffective at low metal concentrations (1–100 mgL⁻¹), generate hazardous by-products, and can be prohibitively expensive when treating large volumes of wastewater (Ahmed et al., 2022; Singh et al., 2012). Effluents from industries such as leather tanning, mining, and electroplating typically contain heavy metals at low concentrations (1–20 mgL⁻¹) (Chen et al., 2012). These toxic metals pose serious ecological and human health risks due to their bioaccumulation and biomagnification in food chains. Consequently, there is a growing interest in developing efficient, eco-friendly, and cost-effective treatment strategies for low-metal-content wastewater.

The use of growing microalgal cells for metal detoxification offers a sustainable solution. Microalgae can mitigate metal toxicity while simultaneously providing environmental benefits such as oxygen generation for heterotrophic organisms and organic compound excretion, which facilitates metal chelation (Perez-Garcia et al., 2011). Although most recent studies have focused on biosorption using non-living biomass, bioaccumulation by live microalgae remains underexplored (Chen et al., 2012; Areco et al., 2012). This study investigates the metal resistance, removal efficiency, and localization

patterns of *Chlorella minutissima* (*C. minutissima*) when exposed to Cd²⁺, Cr⁶⁺, Pb²⁺, and Zn²⁺ metals chosen for their high toxicity and prevalence in industrial effluents (Dheri et al., 2007; Khurana et al., 2003). *C. minutissima* was selected due to its advantageous morphological features (unicellular, spherical), adaptability to sewage wastewater (Singh et al., 2012), and ability to grow heterotrophically (Bhatnagar et al., 2010). The findings aim to inform the development of scalable algal-based systems for treating low-metal-content industrial wastewater.

Materials and methods

Biological samples were grown in a clean, sterile container under controlled conditions to maintain its viability and culture until further used for growth kinetics and heavy metal degradation. All chemicals used were of analytical grade and were used as received without any further purification. All experimental treatments, including controls, were performed in triplicate (n = 3), and results are expressed as mean ± standard deviation (SD).

Algal Stock Cultures and Inoculum Preparation

The microalga *Chlorella minutissima* used in this study was obtained from our laboratory culture collection (Department of Chemical Engineering, Dr. B.R. Ambedkar National Institute of Technology, Jalandhar, Punjab, India), originally procured from Indian Agricultural Research Institute (IARI), New Delhi, as reported earlier (Singh et al., 2011; Singh et al., 2012). The strain was maintained axenically in BG-11 medium (Rippka et al., 1979). Identification was based on morphological features using phycological keys, and taxonomic confirmation was cross-checked with published literature. Cultures were incubated at 27 ± 1°C under continuous aeration (1 vvm sterile air) and illuminated with cool white fluorescent lamps at an intensity of 2000–2500 lux, following a 14:10 h light: dark cycle using a tissue culture rack (Vista Biocell Pvt. Ltd., India).

Inoculums density was adjusted to achieve an initial cell concentration of 2 to 4 × 10⁶ cells mL⁻¹ in experimental flasks. Cell numbers were counted using a hemocytometer (Fein-optic, Germany) under an inverted microscope, and correlated with absorbance readings at 686 nm measured every 12 h using a spectrophotometer (SMART Spectro, LaMotte Company, USA). The specific growth rate (μ) was calculated according to Shuler & Kargi (2002) in equation (1):

$$\text{GrowthRate}(k) = \frac{(\log_{10} X_t - \log_{10} X_0)}{\Delta t} \quad (1)$$

Where, X₀ = Initial cell number; X_t = Cell number at time t; Δt = time interval

Synthetic wastewater preparation

Synthetic wastewater used in this study was formulated to mimic nutrient and ionic strength of real effluents, following protocols similar to Ge et al. (2013) for microalgal cultivation in synthetic high-strength wastewater. It was prepared in acid-washed 5 L glass bottles and contained the following components:

- MgSO₄·7H₂O: 1000 mgL⁻¹
- CaCl₂: 84 mgL⁻¹
- Trace element solution: 0.5 mL, consisting of H₃BO₃ (57 mgL⁻¹), FeSO₄·7H₂O (25 mgL⁻¹), ZnSO₄·7H₂O (44 mgL⁻¹), MnCl₂·4H₂O (7 mgL⁻¹), MoO₃ (35 mgL⁻¹), CuSO₄·5H₂O (8 mgL⁻¹), Cu(NO₃)₂·6H₂O (2.5 mgL⁻¹), and NaHCO₃ (2500 mgL⁻¹).

After autoclaving (120°C for 15 min), the pH was adjusted to 7.5 using 0.1N NaOH or 0.1N HCl (Digital pH meter 335, Systronics, Ahmedabad, India). NH₄Cl (1000 mgL⁻¹ stock) and K₂HPO₄ (1000 mgL⁻¹ stock) served as nitrogen and phosphorus sources, respectively.

Metal stock solutions and analysis

Analytical-grade salts of Cd, Cr, Pb, and Zn (Merck Chemicals, India) were used to prepare 1000 mgL⁻¹ stock solutions in accordance with standard protocols (Eaton et al., 2005). Working solutions were prepared by diluting the stock with double-distilled water to achieve the desired concentrations in synthetic wastewater. Metal stock solutions were prepared

using analytical grade CdCl_2 , $\text{K}_2\text{Cr}_2\text{O}_7$, $\text{Pb}(\text{NO}_3)_2$, and $\text{ZnSO}_4 \cdot 7\text{H}_2\text{O}$ dissolved in Milli-Q water, filter-sterilized (0.22 μm), and stored at 4 °C. Working concentrations were obtained by aseptic addition of appropriate volumes of stock solutions to sterile culture flasks. The pH was adjusted to 7.5 prior to inoculation to minimize precipitation and ensure metal solubility. Residual concentrations of Cd^{2+} , Pb^{2+} , and Zn^{2+} were determined using LaMotte Wastewater Analysis Kits (LaMotte Company, USA), based on colorimetric detection (dithizone method for $\text{Cd}^{2+}/\text{Pb}^{2+}$ and zincon method for Zn^{2+}). Absorbance was recorded with a LaMotte SMART3 colorimeter, and all measurements were performed in triplicate. The manufacturer-reported detection limits were 0.05 mgL^{-1} (Cd^{2+}), 0.1 mgL^{-1} (Pb^{2+}), and 0.01 mgL^{-1} (Zn^{2+}). Blanks were analyzed alongside each sample set to ensure reliability. Calibration was performed using standard solutions supplied with the LaMotte kits prior to each experimental run. Chromium speciation was determined using the diphenylcarbazide method (ASTM D6832-08; ASTM, 2010). Cr^{6+} concentrations were measured colorimetrically at 540 nm, while total Cr was analyzed after acid digestion. Cr^{3+} concentrations were obtained by subtracting Cr^{6+} from total chromium. All measurements were performed in triplicate. Spiked recovery experiments demonstrated recoveries of 90–105%, validating method accuracy. Spiked recovery experiments demonstrated recoveries of 90–105%, validating method accuracy.

Growth optimization in synthetic wastewater

Optimization of growth parameters (pH, temperature, biomass dosage) under controlled synthetic media was guided by procedures as described in Sultana et al. (2020). Prior to metal exposure experiments, algal cells were grown in BG-11 media for 7 days under standard growth conditions (27 ± 1 °C, 2000–2500 lux light intensity, 14:10 h light: dark cycle, 1 vvm aeration). Cultures were then acclimated to experimental conditions for 48 h and harvested during the exponential growth phase to ensure consistent physiological status before treatments. The growth response of *C. minutissima* was examined under varying conditions to determine optimal parameters: initial $\text{NH}_4^+ - \text{N}$ (20, 40, 60, 80, 100 and 200 $\text{mg NH}_4^+ - \text{NL}^{-1}$) and $\text{PO}_4^{3-} - \text{P}$ (5, 10, 20, 50, 75 and 100 $\text{mg PO}_4^{3-} - \text{PL}^{-1}$) concentrations, light: dark (h: h) duration (18:6, 14:10 and 12:12), pH range; adjusted pH and unadjusted pH (5.5 6.5 and 7.5) and D-glucose concentration (10, 50, 100, 150, and 200 mg glucose L^{-1}) were studied. The effect of pH was studied under both unadjusted (natural medium pH) and adjusted conditions, with pH values set at 5.5, 6.5, and 7.5. Biomass concentration was determined spectrophotometrically at 680 nm (OD_{680}) using a UV-Vis spectrophotometer (Shimadzu UV-1800, Japan). A calibration curve was prepared by correlating OD_{680} with cell dry weight, obtained by filtering 10 mL of culture through pre-weighed GF/C filters and drying at 105 °C to constant weight. Biomass values are reported as mgL^{-1} dry weight. Chlorophyll *a* content was estimated according to standard spectrophotometric methods (Becker, 1994) only in optimization experiments to assess photosynthetic activity, but not for biomass quantification during metal removal assays.

Metal exposure experiments

Metal exposure concentrations and uptake kinetics are comparable to previously reported chromium exposure studies in microalgae where dose-dependent uptake was observed (Dao et al., 2018). Exponentially growing *Chlorella* cells were exposed to various concentrations of different metal ions and analyzed for growth and metal removal potential in synthetic wastewater. Metal ion concentrations (0.5, 1.0, 3.0, 5.0, and 10.0 mgL^{-1}) were selected based on reported ranges in industrial effluents and polluted water bodies (Dheri et al., 2007; Khurana et al., 2003; Koju et al., 2022). The lower concentrations simulate trace contamination levels, while the higher concentrations approach toxicity thresholds, enabling evaluation of both bioremediation efficiency and tolerance capacity of *C. minutissima*. An initial *C. minutissima* inoculum of $2\text{--}4 \times 10^6$ cells mL^{-1} was inoculated aseptically to 250 mL flasks containing 100 mL synthetic wastewater and supplemented with various concentrations of Cd^{2+} , Cr^{6+} , Pb^{2+} , and Zn^{2+} metals separately. All experiments were carried out in triplicates with control for 13 days at 27 ± 1 °C under most favorable conditions from section 2.4. At the end of the incubation period, the experimental flask was filtered and washed by distilled water for further left over metal detection. Control experiments were run in parallel for each treatment. Negative controls consisted of *C. minutissima* cultures grown under identical conditions without metal addition, to assess baseline growth and biomass production. No separate positive control (reference toxicant) was employed; however, chromium (VI) reduction was validated against the diphenylcarbazide method (ASTM, 2010) as a methodological control.

Influence of metal ions exposure on *C. minutissima* growth

Effect of different concentration of Cd^{2+} , Cr^{6+} , Pb^{2+} , and Zn^{2+} metal ions on *C. minutissima* growth was studied. Specific growth rate of algal cells was calculated by equation (1). Percentage growth inhibition (% I) at each test concentration after 13 days was calculated as follows (ASTM, 2006) in equation (2).

$$I(\%) = \frac{(C - X) 100}{C} \quad (2)$$

Where, C = Average specific growth rate of control; X= Average specific growth rate of an individual test concentration

Bioremoval, bioabsorption and bioadsorption analysis of metal ions

Following 13 days of metal exposure, cultures were centrifuged at 5000 rpm for 10 min (Kubota KS-5200C refrigerated). Supernatants were collected, and algal pellets were washed three times with 20 mM EDTA to desorb surface-bound metals. Metal content was determined in:

1. **Supernatant** – representing unbound extracellular metal.
2. **EDTA wash** – representing surface-adsorbed metal (bioadsorption).
3. **Pellet after EDTA wash** – representing intracellularly absorbed metal (bioabsorption).

Samples were digested with HNO₃ (70%), H₂O₂ (30%), and deionized water (1:1:3) (Bates et al., 1982) and analyzed for metal content. Bioremoval, bioabsorbed and bioadsorbed percentages were calculated according to modified methods from June et al. (2010) and Pérez-Rama et al. (2002) in equation (3), (4), (5) respectively.

$$\begin{aligned} \% \text{ Bioremoval of metal ions in medium} \\ &= \frac{(\text{Initial concentration} - \text{Mean concentration of metal ions in supernatant})}{\text{Initial concentration}} \\ &\times 100 \end{aligned} \quad (3)$$

$$\begin{aligned} \% \text{ Bioabsorbed of metal ions in algal cells} \\ &= \frac{\text{Mean concentration of metal ions in the washed pellet}}{\text{Initial concentration}} \times 100 \end{aligned} \quad (4)$$

$$\begin{aligned} \% \text{ Bioadsorbed of metal ions in algal cells} \\ &= \frac{\text{Mean concentration of metal ions in the EDTA washings}}{\text{Initial concentration}} \times 100 \end{aligned} \quad (5)$$

Cr⁶⁺ Bioreduction

To quantify Cr⁶⁺ reduction to Cr³⁺, the diluted acid-digested fractions (supernatant, EDTA wash, and EDTA-washed pellets) obtained from Section 2.5.2 was each divided into two equal portions. These portions were used to determine the extent of Cr⁶⁺ bioreduction by *C. minutissima*.

In the first portion, Cr³⁺ present in the sample was oxidized back to Cr⁶⁺ (convert Cr³⁺ back to Cr⁶⁺) using potassium permanganate, following ASTM (2010) procedures. This oxidized fraction was used to quantify the total Cr⁶⁺ content for evaluating bioremoval and localization in the microalgal cells. The second portion was left un-oxidized and analyzed directly for Cr⁶⁺. In both cases, Cr⁶⁺ concentrations were determined spectrophotometrically using the diphenylcarbazide method (Eaton et al., 2005).

The amount of Cr⁶⁺ reduced to Cr³⁺ in each compartment—the culture medium (supernatant), the cell surface (EDTA washings), and the intracellular protoplasm (washed pellet)—was calculated by subtracting the unoxidized Cr⁶⁺ value from the corresponding oxidized Cr⁶⁺ value. Total bioreduction per treatment was obtained by summing the amounts reduced across all three compartments. Bioreduction percentages in the medium, protoplasm, cell wall, and overall were calculated using the formula described by June et al. (2010) and Pérez-Rama et al. (2002) in equation (6), (7), (8) and (9).

$$\% \text{ Cr Bioreduction in medium} = \frac{(\text{Oxidized supernatant} - \text{Unoxidized supernatant})}{\text{Oxidized supernatant}} \times 100 \quad (6)$$

$$\begin{aligned} \% \text{ Bioreduction in algal cell protoplasm} \\ &= \frac{(\text{Oxidized washed pellet} - \text{Unoxidized washed pellet})}{\text{Oxidized washed pellet}} \times 100 \end{aligned} \quad (7)$$

$$\% \text{ Bioreduction on the algal cell wall} = \frac{(\text{Oxidized EDTA washing} - \text{Unoxidized EDTA washing})}{\text{Oxidized EDTA washing}} \times 100 \quad (8)$$

$$\begin{aligned} \% \text{ Total Bioreduction} &= \frac{(\text{Sum of all oxidized fractions} - \text{Sum of all unoxidized fractions})}{\text{Sum of all oxidized fractions}} \\ &\times 100 \end{aligned} \quad (9)$$

Statistical analysis

All experiments were performed in triplicate ($n = 3$), and data are presented as mean \pm standard deviation (SD). Statistical analyses were conducted using SPSS v.25 (IBM Corp., USA). One-way ANOVA followed by Tukey's HSD test was applied to determine significant differences among treatments at a 95% confidence level ($p < 0.05$). Regression analysis was used to examine correlations between initial metal concentrations and removal efficiencies. Outliers, identified as values lying beyond $1.5 \times \text{IQR}$, were excluded only when attributable to experimental error. Graphs were plotted using OriginPro 2021 (OriginLab Corp., USA).

Results

Growth Optimization of *C. minutissima*

Effect of initial $\text{NH}_4^+ - \text{N}$ and $\text{PO}_4^{3-} - \text{P}$ concentrations

Specific growth rate patterns of *C. minutissima* at varying concentrations $\text{NH}_4^+ - \text{N}$ (20, 40, 60, 80, 100 and 200 mg $\text{NH}_4^+ - \text{N L}^{-1}$) concentrations were similar (Figure 1a). A one-day lag phase was followed by exponential growth for approximately three days, after which growth gradually declined. The highest average specific growth rate (μ_{max}) was $0.38 \pm 0.04 \text{ d}^{-1}$ at 80 mg L^{-1} , decreasing to $0.20 \pm 0.03 \text{ d}^{-1}$ at 200 mg L^{-1} . Biomass yield increased with ammonium concentration up to 80 mg L^{-1} , which was significantly higher than at both 20 and 200 mg L^{-1} ($p < 0.05$). Thus, 80 mg L^{-1} was selected for subsequent experiments.

At varying $\text{PO}_4^{3-} - \text{P}$ (5, 10, 20, 50, 75 and $100 \text{ mg PO}_4^{3-} - \text{P L}^{-1}$) concentrations, μ_{max} values showed irregular patterns (Figure 1b), decreasing from $0.08 \pm 0.01 \text{ d}^{-1}$ at 5 mg L^{-1} to $-0.005 \pm 0.004 \text{ d}^{-1}$ at 100 mg L^{-1} . Optimal phosphate supplementation (30 mg L^{-1}) supported significantly greater growth compared to 5 and 100 mg L^{-1} ($p < 0.05$). A concentration of 10 mg L^{-1} was selected for further testing.

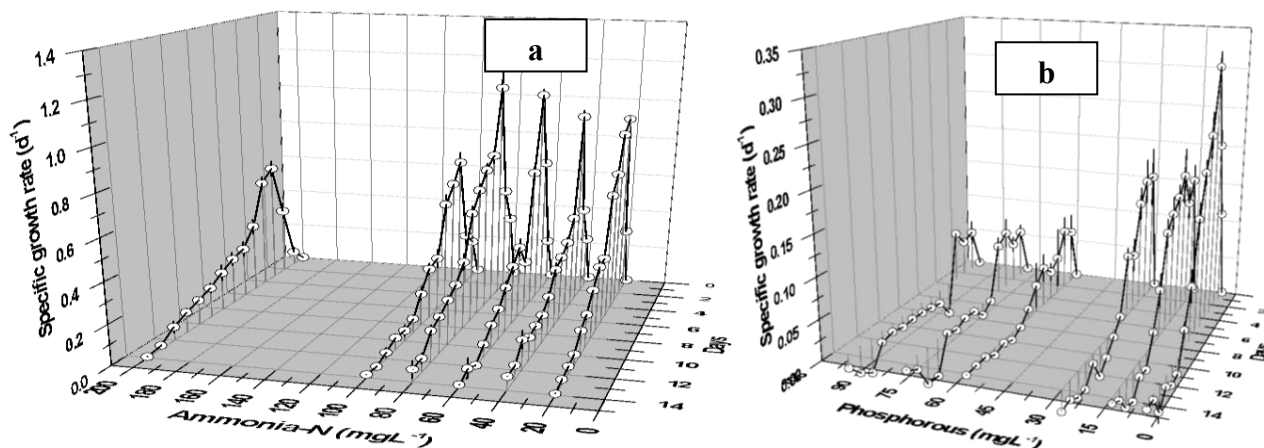


Figure 1. Effect of initial (a) $\text{NH}_4^+ - \text{N}$; and (b) $\text{PO}_4^{3-} - \text{P}$ concentration on specific growth rate of *C. minutissima*

Effect of pH

Each algal species has a definite pH range (normally 5 – 10) for growth (Becker, 1994). Thus, effect of initial medium pH on *C. minutissima* growth rate was analyzed in pH range 5.5 to 7.5. Unadjusted pH experiments (Figure 2a) showed lowest

average specific growth rate ($0.06 \pm 0.01 \text{ d}^{-1}$) at pH 5.5, with cultures reaching death phase by day 9–10. At pH 7.5, growth reached $0.11 \pm 0.009 \text{ d}^{-1}$ with death phase at day 11–12. The highest growth ($0.16 \pm 0.01 \text{ d}^{-1}$) occurred at pH 6.5, with cultures remaining viable throughout the 14-day period. Biomass productivity under adjusted pH 7.5 was significantly higher than under unadjusted pH 5.5 and 6.5 ($p < 0.05$).

Daily pH variation patterns are shown in Figure 2b. In pH-adjusted experiments (Figure 2c), the highest μ_{max} was $0.26 \pm 0.03 \text{ d}^{-1}$ at pH 7.5 ($p < 0.05$), while the lowest ($0.04 \pm 0.008 \text{ d}^{-1}$) was at pH 5.5. Adjusted pH 7.5 was selected for further studies.

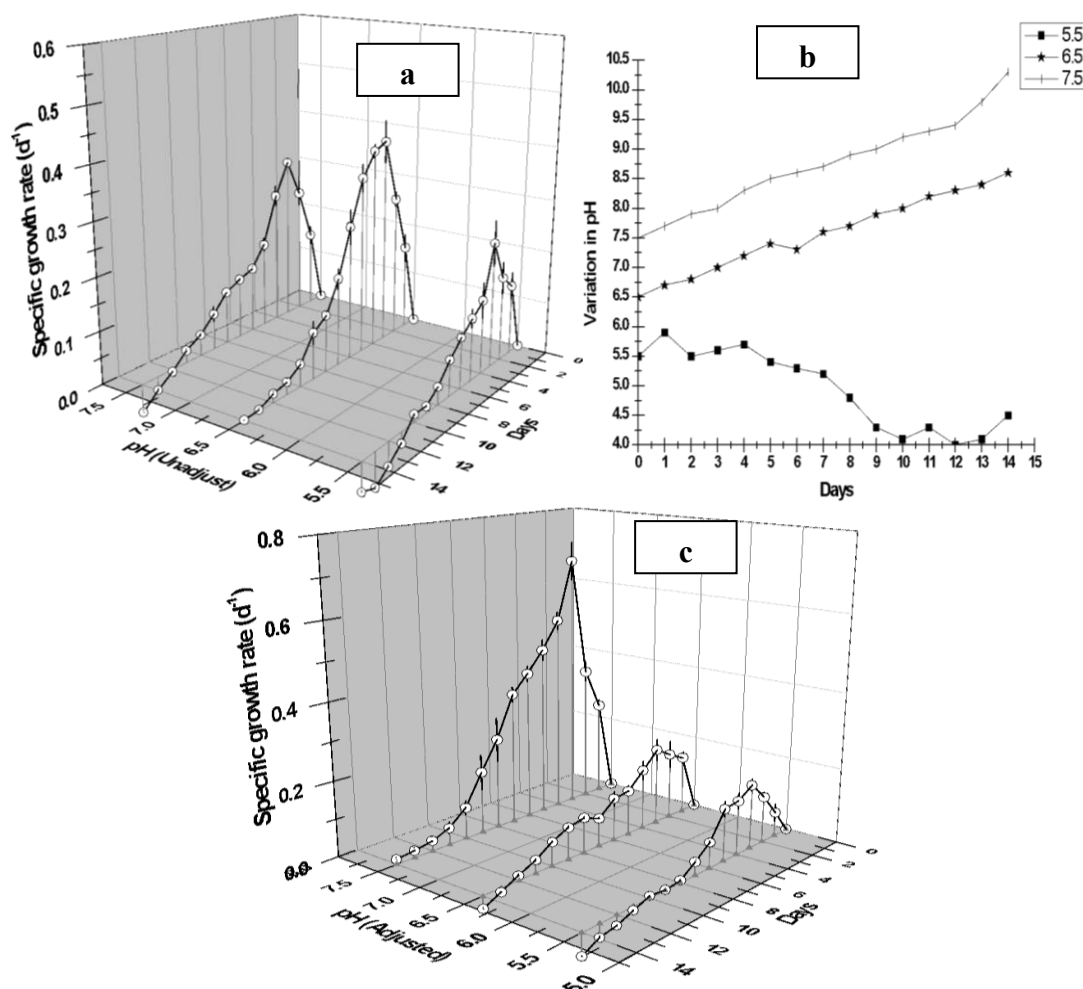


Figure 2. Effect of initial pH (a) Unadjusted; (b) Daily variations in initial pH values of pH (Unadjusted) and (c) Adjusted on specific growth rate of *C. minutissima*

Effect of light duration

Light regime is an important regulatory factor for algal growth kinetics. Many previous studies have shown that the light utilization efficiency is strongly dependent on the light:dark cycles to which algal cultures are subjected (Janssen, M. G. J, 2002). Light:dark cycles of 18:6, 14:10, and 12:12 h were tested (Figure 3). The lowest growth rate ($0.15 \pm 0.02 \text{ d}^{-1}$) occurred at 18:6, the highest ($0.37 \pm 0.03 \text{ d}^{-1}$) at 14:10, and intermediate growth ($0.29 \pm 0.01 \text{ d}^{-1}$) at 12:12. Optimal growth occurred under a 14:10 h light:dark cycle, which was significantly better than both 18:6 and 12:12 cycles ($p < 0.05$). The 14:10 cycle was selected for further experiments.

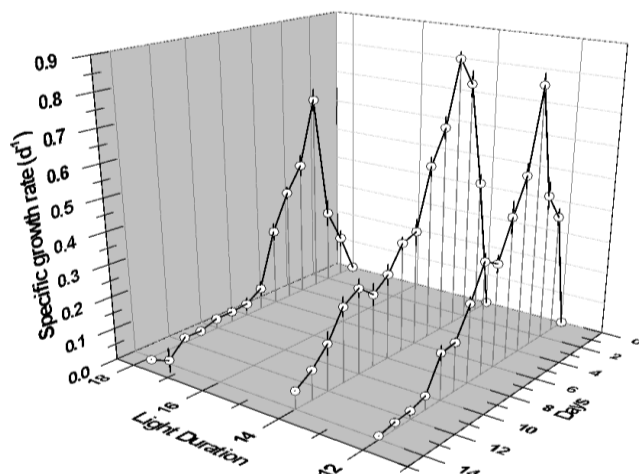


Figure 3. Effect of light duration on specific growth rate of *C. minutissima*

Effect of D-Glucose concentration

Mixotrophic growth potential of *C. minutissima* was evaluated in 100 mL synthetic wastewater supplemented with 10, 50, 100, 150 and 200 mg D-glucose L⁻¹. Glucose supplementation from 10 to 200 mgL⁻¹ affected growth rates as shown in Figure 4. The highest μ_{\max} (0.36 ± 0.22 d⁻¹) occurred at 100 mgL⁻¹, with lower rates at both lower and higher concentrations. The lowest growth (0.19 ± 0.02 d⁻¹) was observed at 200 mgL⁻¹. Cultures supplied with 100 mg L⁻¹ glucose showed significantly higher biomass yield than 10 and 50 mg L⁻¹ treatments ($p < 0.05$). A concentration of 100 mgL⁻¹ was used for subsequent metal studies.

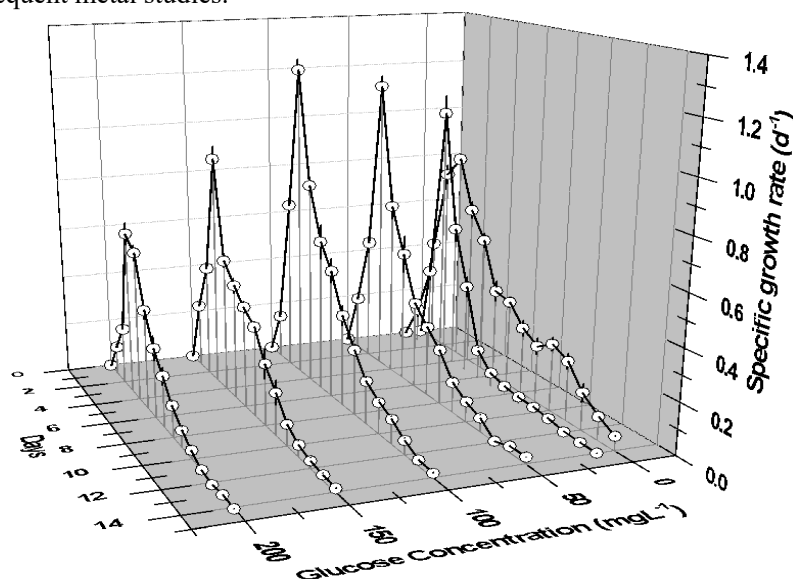


Figure 4. Effect of glucose concentration on specific growth rate of *C. minutissima*

Metal exposure experiments

Growth response to metal ions

Growth profiles of *C. minutissima* in the presence of Cd²⁺, Cr⁶⁺, Pb²⁺, and Zn²⁺ are shown in Figures 5a–d, with corresponding growth inhibition data in Figure 5e and Table 1. At 0.5 mgL⁻¹, average specific growth rates were 0.11 (Cd²⁺), 0.32 (Cr⁶⁺), 0.35 (Pb²⁺), and 0.38 d⁻¹ (Zn²⁺). growth rate at 5 mg L⁻¹ Cd²⁺ was significantly lower than at 0.5 mg L⁻¹ ($p < 0.05$). Increasing metal concentrations resulted in reduced growth, with complete inhibition observed for Cd²⁺ at ≥ 5 mgL⁻¹. Growth inhibition increased proportionally with metal concentration. Growth inhibition was concentration-

dependent, with Cd^{2+} causing significantly higher growth reduction than Pb^{2+} , Cr^{6+} , and Zn^{2+} at equivalent concentrations ($p < 0.05$).

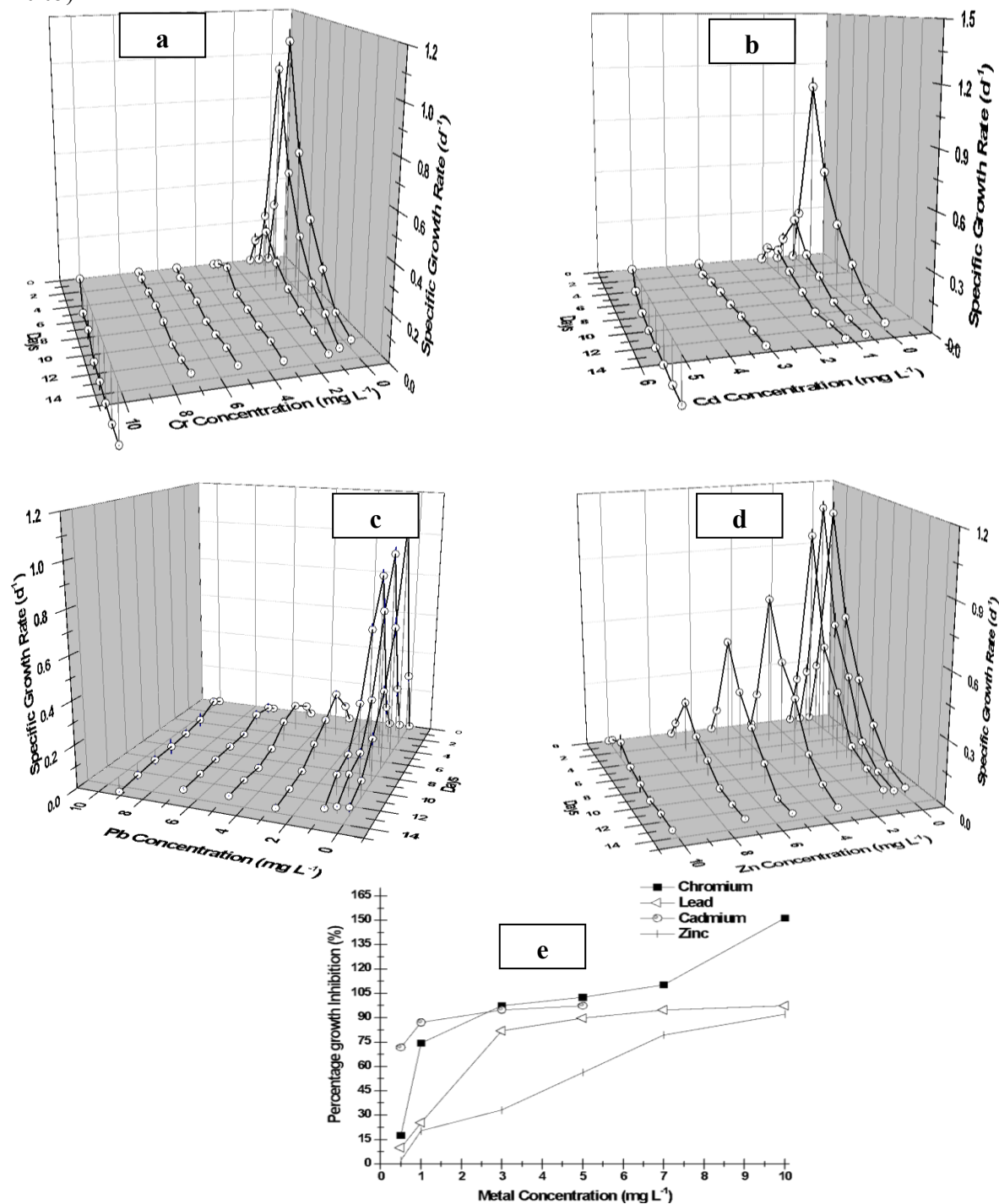


Figure 5. Effect of (a) Cr^{6+} (b) Cd^{2+} (c) Pb^{2+} (d) Zn^{2+} on *C. minutissima* growth rate (e) Percentage growth inhibition in growth rate of *C. minutissima* after 13 days of metal exposure

Table 1. Average specific growth rate (d^{-1}) of *C. minutissima* cells after 13 days exposure to different concentrations of Cadmium, Chromium, Lead and Zinc metal ions (Mean values; n=3)

Metal Concentration (mgL ⁻¹)	Chromium (Cr ⁶⁺)	Lead (Pb ²⁺)	Cadmium (Cd ²⁺)	Zinc (Zn ²⁺)
0.5	0.32	0.35	0.11	0.38
1	0.10	0.29	0.05	0.31
3	0.01	0.07	0.02	0.26
5	-0.01	0.04	0.01	0.17
7	-0.04	0.02	Cell death	0.08
10	-0.20	0.01	Cell death	0.03

Metal Bioremoval, Bioabsorption, and Bioadsorption

Removal of Zn²⁺

The amounts and percentages of Zn²⁺ bioremoval, bioabsorption, and bioadsorption by *C. minutissima* at different concentrations are shown in Figure 6a and Table 2. The lowest bioremoval percentage ($3.2 \pm 0.1\%$, $3.19 \pm 0.07 \mu\text{g}$ per 100 mL) occurred at 10 mg L^{-1} , while the highest percentage ($98.63 \pm 0.63\%$, $4.93 \pm 0.03 \mu\text{g}$ per 100 mL) was obtained at 0.5 mg L^{-1} . The bioremoval % of Zn²⁺ at 0.5 mg L^{-1} is significantly higher than at 3 mg L^{-1} and 10 mg L^{-1} ($p < 0.05$). As shown in Figure 6a, percentage bioremoval decreased with increasing metal concentration; however, the highest removal amount ($7.56 \pm 0.11 \mu\text{g}$ per 100 mL, $25.18 \pm 0.33\%$ bioremoval) was recorded at 3 mg L^{-1} . The highest Zn²⁺ removal percentage ($98.63 \pm 0.63\%$) at 0.5 mg L^{-1} was significantly greater than at 3 mg L^{-1} ($25.18 \pm 0.33\%$) and 10 mg L^{-1} ($3.2 \pm 0.1\%$) ($p < 0.05$).

Similar trends were observed for bioabsorption. The amount of bioabsorbed Zn²⁺ increased from $4.84 \pm 0.03 \mu\text{g}$ per 100 mL at 0.5 mg L^{-1} to a maximum of $7.47 \pm 0.11 \mu\text{g}$ per 100 mL ($24.89 \pm 0.30\%$ bioabsorption) at 3 mg L^{-1} , before sharply declining at higher concentrations. The highest bioabsorption percentage ($96.9 \pm 0.70\%$) occurred at 0.5 mg L^{-1} . At 10 mg L^{-1} , the bioabsorption percentage decreased to $3.1 \pm 0.1\%$ ($313.3 \pm 6.5 \mu\text{g}$ per 100 mL).

Bioadsorption followed a similar pattern to bioremoval and bioabsorption, with the maximum amount ($0.88 \pm 0.09 \mu\text{g}$ per 100 mL, $0.29 \pm 0.35\%$ bioadsorption) observed at 3 mg L^{-1} . The highest bioadsorption percentage ($1.68 \pm 0.25\%$, $0.08 \pm 0.01 \mu\text{g}$ per 100 mL) was recorded at 0.5 mg L^{-1} and decreased only slightly with increasing Zn²⁺ concentration (Figure 6a).

Removal of Pb²⁺

The bioremoval, bioabsorption, and bioadsorption of Pb²⁺ by *C. minutissima* are presented in Figure 6b and Table 2. The lowest bioremoval percentage ($1.5 \pm 0.1\%$, $1.50 \pm 0.08 \mu\text{g}$ per 100 mL) occurred at 10 mg L^{-1} , while the highest ($93.15 \pm 2.5\%$, $4.66 \pm 0.12 \mu\text{g}$ per 100 mL) was achieved at 0.5 mg L^{-1} . Pb²⁺ removal at 0.5 mg L^{-1} ($93.15 \pm 2.5\%$) was significantly higher than at 3 mg L^{-1} ($22.86 \pm 0.22\%$) and 10 mg L^{-1} ($1.5 \pm 0.1\%$) ($p < 0.05$). Bioremoval amounts increased gradually from $4.66 \pm 0.12 \mu\text{g}$ per 100 mL at 0.5 mg L^{-1} to $6.86 \pm 0.06 \mu\text{g}$ per 100 mL ($22.86 \pm 0.22\%$) at 3 mg L^{-1} . The highest bioabsorbed amount ($6.79 \pm 0.07 \mu\text{g}$ per 100 mL, $22.64 \pm 0.25\%$ bioabsorption) was also recorded at 3 mg L^{-1} . The highest bioabsorption percentage ($91.4 \pm 2.66\%$, $4.57 \pm 0.13 \mu\text{g}$ per 100 mL) occurred at 0.5 mg L^{-1} (Figure 6b). Bioabsorption at 3 mg L^{-1} ($6.79 \pm 0.07 \mu\text{g}$ per 100 mL) was significantly greater than at 0.5 and 1 mg L^{-1} ($p < 0.05$).

In contrast, bioadsorption patterns differed from bioremoval and bioabsorption. Both the highest amount ($0.09 \pm 0.01 \mu\text{g}$ per 100 mL) and percentage ($1.7 \pm 0.26\%$) were observed at 0.5 mg L^{-1} , with values decreasing at higher concentrations.

Removal of Cd²⁺

The amounts and percentages of Cd²⁺ bioremoval, bioabsorption, and bioadsorption by *C. minutissima* are summarized in Table 2 and Figure 6c. Both the highest removal percentage ($40.49 \pm 1.98\%$) and amount ($2.02 \pm 0.10 \mu\text{g}$ per 100 mL) occurred at 0.5 mg L^{-1} . Increasing the concentration sharply reduced removal efficiency, with only $0.14 \pm 0.02 \mu\text{g}$ per 100 mL (0.1%) removed at 10 mg L^{-1} . Cell death was observed at $\geq 5 \text{ mg L}^{-1}$. Bioadsorption patterns mirrored bioremoval trends, with a maximum of $1.96 \pm 0.09 \mu\text{g}$ per 100 mL ($39.23 \pm 1.87\%$) at 0.5 mg L^{-1} , followed by steep declines at higher

concentrations. Cd^{2+} removal efficiency at 0.5 mg L^{-1} ($40.49 \pm 1.5\%$) was significantly higher than at 3 and 10 mg L^{-1} ($p < 0.05$).

Bioadsorption trends differed slightly. The highest amount ($0.09 \pm 0.03 \text{ } \mu\text{g}$ per 100 mL , $0.90 \pm 0.27\%$ bioadsorption) occurred at 1.0 mg L^{-1} , while the highest bioadsorption percentage ($1.27 \pm 0.10\%$, $0.06 \pm 0.05 \text{ } \mu\text{g}$ per 100 mL) was observed at 0.5 mg L^{-1} . At higher concentrations ($\geq 5 \text{ mg L}^{-1}$), growth was significantly inhibited compared to controls ($p < 0.05$) Beyond 1.0 mg L^{-1} , bioadsorption declined gradually with increasing metal concentration.

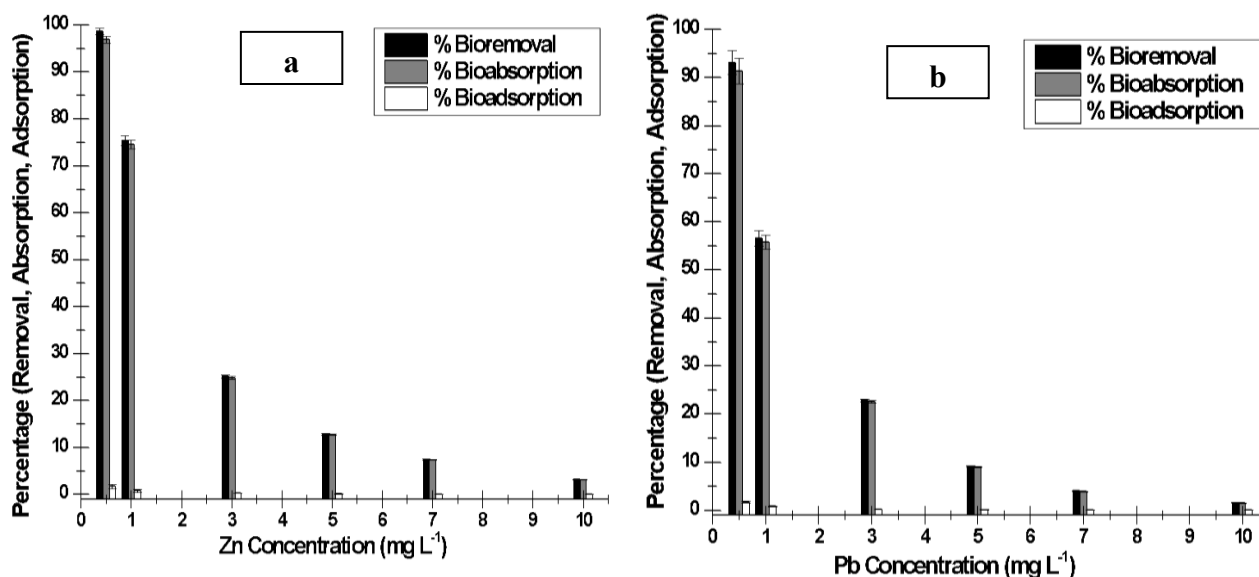
Removal of Cr^{6+}

The bioremoval, bioabsorption, and bioadsorption data for Cr^{6+} by *C. minutissima* at different concentrations are presented in Figure 6d and Table 2. The lowest bioremoval percentage ($0.6 \pm 0.1\%$, $0.60 \pm 0.05 \text{ } \mu\text{g}$ per 100 mL) occurred at 10 mg L^{-1} , while the highest percentage ($85.69 \pm 2.2\%$, $4.28 \pm 0.11 \text{ } \mu\text{g}$ per 100 mL) was recorded at 0.5 mg L^{-1} . In contrast, the highest bioremoval amount ($5.89 \pm 0.06 \text{ } \mu\text{g}$ per 100 mL , $19.66 \pm 0.22\%$) was obtained at 3 mg L^{-1} . Bioabsorption followed similar trends, with the lowest amount ($0.57 \text{ } \mu\text{g}$ per 100 mL , $0.6 \pm 0.1\%$) at 10 mg L^{-1} and the highest amount ($5.74 \pm 0.11 \text{ } \mu\text{g}$ per 100 mL , $19.13 \pm 0.37\%$) at 3 mg L^{-1} . The highest bioabsorption percentage ($84.0 \pm 1.96\%$, $4.20 \pm 0.09 \text{ } \mu\text{g}$ per 100 mL) occurred at 0.5 mg L^{-1} . Cr^{6+} removal percentage at 0.5 mg L^{-1} ($85.69 \pm 2.1\%$) was significantly greater than at 10 mg L^{-1} ($15.2 \pm 1.2\%$) ($p < 0.05$).

Bioadsorption patterns differed slightly. The maximum amount ($0.20 \pm 0.04 \text{ } \mu\text{g}$ per 100 mL , $1.6 \pm 0.35\%$ bioadsorption) was recorded at 1.0 mg L^{-1} , whereas the highest bioadsorption percentage ($1.68 \pm 0.25\%$, $0.08 \pm 0.01 \text{ } \mu\text{g}$ per 100 mL) occurred at 0.5 mg L^{-1} . Bioadsorption decreased gradually with increasing Cr^{6+} concentration (Figure 6d).

Cr^{6+} bioreduction

The capacity of *C. minutissima* to bioreduce Cr^{6+} to Cr^{3+} at different initial concentrations is summarized in Table 3 and Figure 6e. Total bioreduction amounts increased from $4.56 \text{ } \mu\text{g mL}^{-1}$ at 0.5 mg L^{-1} to a maximum of $8.26 \text{ } \mu\text{g mL}^{-1}$ at 3 mg L^{-1} , followed by a decline to $1.86 \text{ } \mu\text{g mL}^{-1}$ at 10 mg L^{-1} . The highest bioreduction percentage (58%) was observed at 0.5 mg L^{-1} . At lower concentrations (0.5 and 1.0 mg L^{-1}), a greater proportion of the reduced chromium was localized in the protoplasm— 43% and 22% of the total, respectively—compared to the cell wall or medium. The highest Cr^{3+} accumulation in the protoplasm was recorded at 1.0 mg L^{-1} ($5.76 \text{ } \mu\text{g mL}^{-1}$). Bioreduction efficiency was significantly greater at 0.5 mg L^{-1} compared to 10 mg L^{-1} ($p < 0.05$). Bioreduction to Cr^{3+} was significantly higher in the protoplasm than in extracellular fractions ($p < 0.05$). Overall, bioreduction percentages declined steadily from 58% at 0.5 mg L^{-1} to 2.8% at 10 mg L^{-1} , indicating reduced enzymatic reduction efficiency at higher Cr^{6+} levels (Figure 6e).



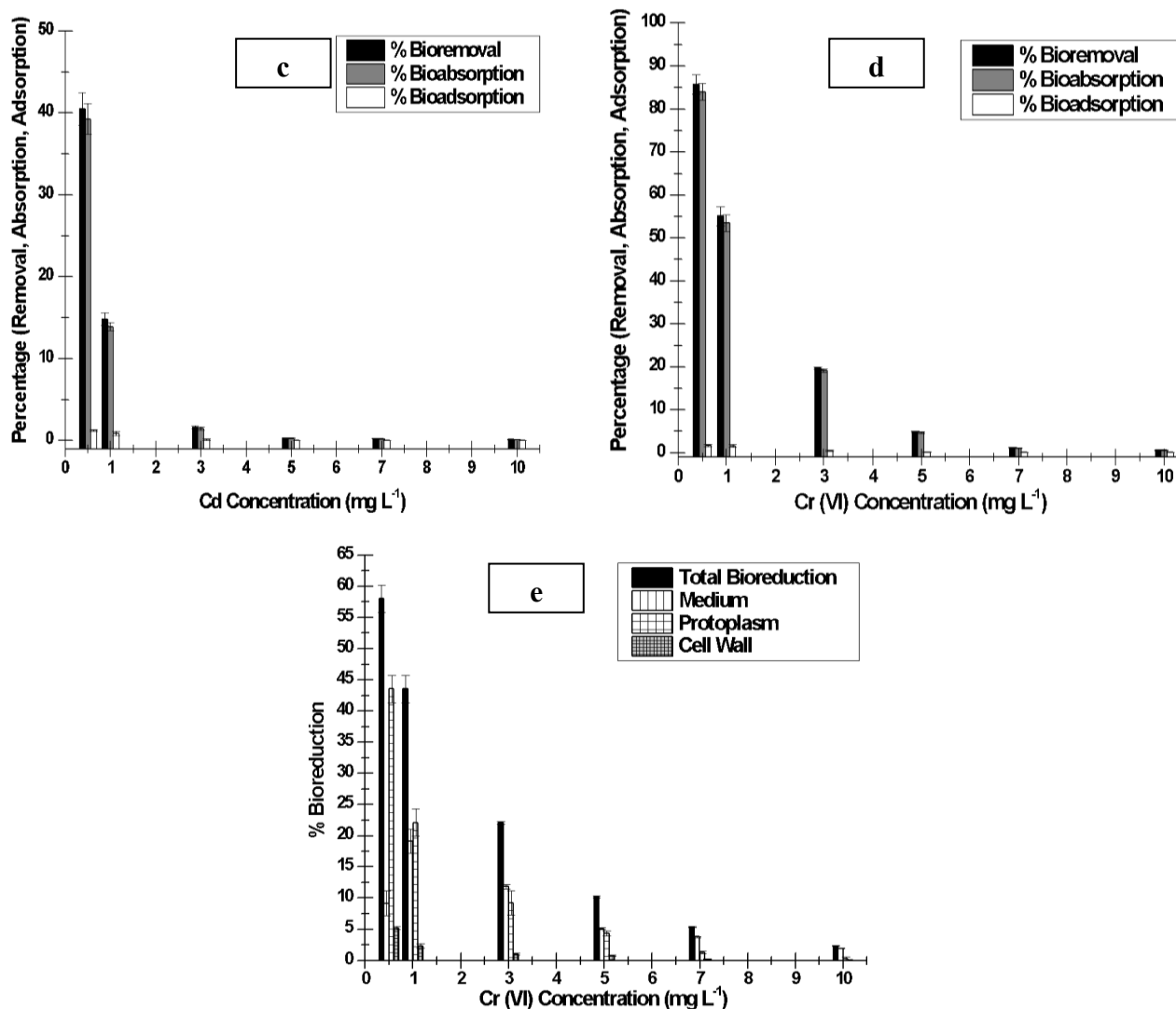


Figure 6. Bioremoval, bioabsorption and bioadsorption of (a) Zn^{2+} , (b) Pb^{2+} , (c) Cd^{2+} , (d) Cr^{6+} ; and (e) Percent Cr^{6+} bioreduction in the test medium, on the cell wall and in the cell protoplasm at various Cr^{6+} concentrations by growing *C. minutissima* after 13 days of metal exposure

Table 2. Bioremoval, bioabsorption and bioadsorption of different concentrations of Cd^{2+} , Cr^{6+} , Pb^{2+} and Zn^{2+} metal ions (Mean values; n=3)

Heavy Metal	Parameter (μgL^{-1}) + SD	0.5 mgL^{-1}	1 mgL^{-1}	3 mgL^{-1}	5 mgL^{-1}	7 mgL^{-1}	10 mgL^{-1}
Chromium (Cr^{6+})	Bioremoval	428.5 + 11.1	550.9 + 22.0	589.9 + 6.7	244.4 + 8.4	83.7 + 6.3	60.8 + 5.2
	Bioabsorption	420.1 + 9.8	534.9 + 19.5	574.0 + 11.1	236.1 + 9.3	76.8 + 6.7	57.4 + 5.1
	Bioadsorption	8.4 + 1.3	16.0 + 3.5	15.9 + 4.4	8.3 + 3.5	7.0 + 1.7	3.4 + 0.3
Lead (Pb^{2+})	Bioremoval	465.7 + 12.4	566.1 + 15.4	686.3 + 6.5	455.4 + 7.5	279.7 + 7.0	154.7 + 8.0
	Bioabsorption	457.1 + 13.3	558.1 + 14.5	679.1 + 7.6	450.1 + 6.6	273.7 + 5.2	148.3 + 8.9
	Bioadsorption	8.62 + 1.3	8.0 + 0.9	7.2 + 1.3	5.3 + 1.3	5.9 + 2.4	6.3 + 0.8
Cadmium (Cd^{2+})	Bioremoval	202.5 + 9.9	148.2 + 7.5	48.9 + 4.9	15.4 + 3.6	17.3 + 1.5	14.0 + 2.0
	Bioabsorption	196.2 + 9.4	139.2 + 4.9	44.4 + 6.5	12.8 + 3.5	14.7 + 2.1	11.3 + 1.9
	Bioadsorption	6.3 + 0.5	9.0 + 2.7	4.5 + 3.0	2.6 + 0.7	2.6 + 1.5	2.7 + 0.3
Zinc (Zn^{2+})	Bioremoval	493.2 + 3.2	753.8 + 10.7	755.5 + 10.2	642.1 + 7.7	523.3 + 6.0	318.7 + 7.0
	Bioabsorption	484.4 + 3.5	745.8 + 9.1	746.8 + 10.7	635.5 + 6.8	517.1 + 5.7	313.3 + 6.5
	Bioadsorption	8.7 + 2.4	8.01 + 3.6	8.785 + 0.9	6.6 + 1.9	6.3 + 1.0	5.3 + 1.9

Table 3. The amount of Cr⁶⁺bioremoved and bioreduced in the test media, on the algal cell wall and inside protoplasm at different initial Cr⁶⁺ concentration growing *C. minutissima* after 13 days of metal exposure (Mean values; n=3)

Cr ⁶⁺ (mgL ⁻¹)	Total bioremoval (µg mL ⁻¹)	Bioreduction (µg mL ⁻¹)	Media (µg mL ⁻¹)	Protoplasm (µg mL ⁻¹)	Cell wall (µg mL ⁻¹)
0.5	4.28	4.56	0.15	3.56	0.85
1	5.50	7.35	0.83	5.76	0.76
3	5.89	8.26	2.28	4.93	1.05
5	2.44	4.12	2.22	1.67	0.23
7	0.83	2.53	1.75	0.63	0.15
10	0.60	1.86	1.38	0.32	0.16

Discussion

Efficacy of *C. minutissima* in heavy metal bioremediation

The integration of algal cultivation with wastewater treatment processes offers a dual benefit: effective pollutant removal and the generation of valuable biomass for downstream applications, aligning with principles of a circular bioeconomy (Salama et al., 2019). The results of this study confirm that *C. minutissima*, a freshwater microalga, possesses strong potential as a sustainable, low-cost bioremediation agent for industrial effluents contaminated with heavy metals. This aligns with previous findings demonstrating the capacity of *Chlorella* species to tolerate and detoxify wastewater containing toxic metals while producing biomass of commercial value (Bhatnagar et al., 2010; Malla et al., 2015; Singh et al., 2011). Compared to conventional physicochemical treatment methods, which often produce toxic sludge and incur high costs (Jyoti & Awasthi, 2014), algal-based systems offer an environmentally friendly alternative with added value through biomass utilization.

Optimal growth conditions are crucial for maximizing the bioremediation efficiency of *C. minutissima* in industrial effluents (Cao et al., 2014, Saxena et al., 2016). Empirical studies confirm that initial nutrient concentrations, pH, light: dark cycles, and organic carbon supplementation significantly influence algal performance and metal uptake. In our study, *C. minutissima* achieved removal efficiencies of 98.63% for Zn²⁺, 93.15% for Pb²⁺, 85.69% for Cr⁶⁺, and 40.49% for Cd²⁺ at low initial concentrations (0.5 mgL⁻¹). These values are consistent with previous reports of high Zn²⁺ and Pb²⁺ removal efficiencies and moderate to low Cd²⁺ removal due to cadmium's high toxicity (Satoh et al., 2005; Danouche et al., 2022). Cd²⁺ exerted significantly stronger inhibitory effects on growth than Pb²⁺, Cr⁶⁺, or Zn²⁺ (p < 0.05), supporting its ranking as the most toxic metal. Optimal cultivation generally occurs at neutral to slightly alkaline pH values, typically around 7.0 to 7.5, which supports maximal biomass productivity and metabolic activity essential for metal removal. High biomass production by microalgae, such as *C. minutissima*, is recognized as a sustainable alternative for tertiary wastewater treatment (Lavrinovičs & Juhna, 2017). This microalga exhibits robust growth and notable metal removal capabilities, making it a promising alternative to conventional physicochemical treatment methods that often generate problematic sludge and incur high costs.

Influence of environmental and operational parameters

Optimal cultivation conditions were essential to achieve these removal efficiencies. Specific concentrations of nitrogen and phosphorus are crucial for enhancing growth rates and overall biomass composition, including lipids and carbohydrates, which in turn affect metal tolerance and biosorption. Our results support earlier studies showing that neutral to slightly alkaline pH (7.0–7.5), sufficient nitrate (~80 mg L⁻¹) and phosphate (~10 mgL⁻¹) supply, a 14:10 h light: dark photoperiod, and glucose supplementation (~100 mgL⁻¹) enhance *Chlorella* growth and pollutant removal (Cao et al., 2014; Singh et al., 2013). *C. minutissima* has been shown to effectively remove wastewater nutrients like nitrogen (99.19% removal) and phosphorus (96% removal) (Singh et al., 2013).

pH stability is particularly important, as it influences both biomass productivity and the ionic form of metals, thereby affecting biosorption and bioreduction (Cao et al., 2014). An alkaline pH has been identified as particularly suitable for achieving higher biomass production in *C. minutissima* (Saxena et al., 2016). Maintaining a stable optimal pH around 7.5 supports maximal metal uptake and bioreduction, as shifts in pH can alter metal ion charge and binding.

Extended or continuous illumination (e.g., 14:10 h light: dark cycles or 24 hours of light) promotes higher biomass yields and growth rates for *C. minutissima* (Cao et al., 2014). Optimal light conditions are essential for photosynthetic

activity, which powers the metabolic processes involved in metal uptake. Organic carbon supplementation improved mixotrophic growth, resilience to metal stress, and overall bioaccumulation capacity. Similar observations have been made in *Chlorella vulgaris* and *C. minutissima* cultivated under glucose or glycerol-supplemented conditions. Supplementation with organic carbon sources, such as glucose at concentrations around 100 mgL⁻¹ or glycerol at 12.5 gmL⁻¹, can significantly improve mixotrophic growth (Yang et al., 2015; Cao et al., 2014). This enhances algal resilience and bioaccumulation capabilities, supporting effective removal of metals like cadmium, chromium, lead, and zinc, while also promoting the production of biofuel precursors (Yang et al., 2015).

Metal toxicity patterns and physiological responses

The ability of *C. minutissima* to tolerate and remove heavy metals varies depending on the specific metal type and its concentration (Satoh et al., 2005). Studies indicate that at low concentrations (0.5 - 1 mgL⁻¹), algal growth is only slightly inhibited, demonstrating good tolerance to these contaminants. However, at higher concentrations, heavy metals can cause significant physiological stress and growth impairment. The relative toxicity order observed—Cd > Cr > Pb > Zn agrees with previous studies (Satoh et al., 2005; Danouche et al., 2022). This hierarchy is strongly influenced by the physicochemical properties of the metals, which dictate their bioavailability, transport across cell membranes, and subsequent cellular impact (Zhu et al., 2013). Cd²⁺ is generally the most toxic, causing strong growth inhibition even at low concentrations. Cd²⁺ toxicity is linked to its small ionic radius, high electronegativity, and strong affinity for thiol groups, enabling it to disrupt photosynthesis, nitrogen metabolism, and ultrastructure even at minimum levels (Satoh et al., 2005; Kinuthia et al., 2020).

Its small ionic radius, high electronegativity, and strong oxidative potential facilitate its penetration into algal cells and disrupt essential biochemical processes like photosynthesis and nitrogen fixation (Satoh et al., 2005). Severe disruption of cellular ultrastructure and metabolic functions has been reported at concentrations of 5 mgL⁻¹ Cd²⁺ and above. The US EPA's regulatory limit for Cd²⁺ in drinking water is 0.005 ppm, highlighting its extreme toxicity (Kinuthia et al., 2020). Chromium toxicity is intermediate, primarily due to its ability to induce oxidative stress and interfere with membrane transport. The hexavalent form (Cr⁶⁺) is particularly toxic due to its high oxidizing potential and ease of permeation into cells (Singh et al., 2012). Our Cr⁶⁺ bioreduction (85.69%) was significantly higher ($p < 0.05$) than the 60–70% reported for *Chlorella vulgaris* (June et al., 2010), demonstrating species-specific variation in detoxification capacity. Lead exhibits moderate toxicity, generally less severe than Cd and Cr.

Industrial wastewaters can contain large concentrations of lead, causing significant environmental damage (Malakootian et al., 2019). Zinc is typically the least inhibitory among these metals, even at moderate concentrations, consistent with its role as an essential micronutrient at low levels. At 0.5 mgL⁻¹, only minor growth inhibition (2.24%) has been observed. However, Pb²⁺ exhibited the highest uptake amount at 3 mg L⁻¹, while Zn²⁺ showed the highest removal percentage at 0.5 mg L⁻¹. Thus, Pb²⁺ was more efficiently accumulated in absolute terms, whereas Zn²⁺ removal efficiency was greater at lower concentrations. Thus, Cr⁶⁺ toxicity arises from its oxidative potential and ability to cross cell membranes, while Pb²⁺ exerts moderate toxicity and Zn²⁺ remains the least inhibitory due to its role as an essential micronutrient.

Zn²⁺ caused the least inhibitory effect on growth, while Cd²⁺ showed the strongest toxicity, followed by Cr⁶⁺ and Pb²⁺. Cd²⁺ caused the strongest inhibition of algal growth ($p < 0.05$), confirming its high toxicity, while Zn²⁺ achieved the highest removal percentage at low concentrations, highlighting its efficient bioremoval despite lower uptake amounts compared to Pb²⁺. Overall, significantly higher removal at 0.5 mg L⁻¹ compared to 10 mg L⁻¹ ($p < 0.05$) indicates that *C. minutissima* is particularly effective at treating effluents containing trace levels of heavy metals. Metal stress responses in *C. minutissima* included reduced growth rates at higher concentrations, likely due to reactive oxygen species (ROS) generation, lipid peroxidation, and chloroplast damage, which impair photosynthesis and cell division (McKay & Porter, 1997; Olasehinde et al., 2019). Heavy metal exposure can lead to disruption of chloroplast ultrastructure, reduced chlorophyll content, impaired photosynthetic efficiency, and compromised cell division.

Mechanisms of metal removal

Bioremoval experiments generally show that the percentage of metal removed decreases with increasing metal concentration, while the absolute amount removed may peak at intermediate concentrations. This phenomenon is attributed to the saturation of available binding sites on the algal biomass and reduced metabolic activity at higher toxicant levels (Jais et al., 2017). Thus, *C. minutissima* employs sophisticated mechanisms for heavy metal removal,

which can be broadly described by a two-phase uptake model. Our findings also fit the well-established two-phase uptake model (Monteiro et al., 2012). The two-phase model involves initial rapid extracellular bioadsorption followed by slower active intracellular bioabsorption.

- *Extracellular Bioadsorption* – This is the initial, rapid, and passive phase of metal uptake, occurring within minutes to hours (Novák et al., 2020). Heavy metals bind to functional groups (carboxyl, hydroxyl, amino, phosphate) present on the microalgal cell wall, such as polysaccharides, proteins, and extracellular polymeric substances (EPS) (Spain et al., 2021). This process is largely physicochemical, involving ion exchange and complexation, and does not require metabolic energy (Monteiro et al., 2012).
- *Intracellular Bioabsorption* – Following adsorption, metals are actively transported into the cytoplasm of cell through energy-dependent pathways (Monteiro et al., 2012). This phase is slower but contributes significantly to the total metal removal, especially at lower metal concentrations where cellular metabolism is not severely inhibited (Owen et al., 2010). Intracellular processes include sequestration, detoxification, and storage within cellular compartments, often involving metal-binding proteins like metallothioneins and phytochelatins (Luo, 2003).

The predominance of extracellular versus intracellular pathways is influenced by several factors, including metal concentration, microalgal species, exposure duration, and environmental conditions. For instance, at low metal concentrations and shorter exposure times, extracellular adsorption may dominate due to rapid surface binding (Novák et al., 2020). However, with prolonged exposure and moderate toxicity, intracellular absorption becomes more significant. In cases of severe toxicity, such as with high Cd^{2+} concentrations, the inhibition of cell metabolism can limit intracellular uptake, causing extracellular adsorption to become the primary or only effective removal pathway (Owen et al., 2010). Mallick & Rai (1993) showed that for specific metals, *C. minutissima* has demonstrated remarkable removal efficiencies:

- Zn^{2+} : The highest percentage removal (98.63%) was observed at a low concentration of 0.5 mg/L, while the maximum absolute removal amount ($7.56 \mu\text{g}/100 \text{ mL}^{-1}$) was achieved at 3 mgL^{-1} (Mallick & Rai, 1993). Our Zn^{2+} removal (98.63%) was significantly greater ($p < 0.05$) than values reported for *Ulva lactuca* (Areco et al., 2012), confirming the superior efficiency of *C. minutissima*.
- Pb^{2+} and Cr^{6+} : Similar patterns of removal percentage decreasing with increasing concentration, but absolute amount peaking at intermediate concentrations ($1\text{--}3 \text{ mgL}^{-1}$), were observed for Pb^{2+} and Cr^{6+} (Mallick & Rai, 1993).
- Cd^{2+} : Due to its pronounced toxicity, Cd^{2+} toxicity was significantly greater ($p < 0.05$) than Pb^{2+} and Zn^{2+} , in agreement with prior studies (Mallick & Rai, 1993; Monteiro et al., 2012). Cd^{2+} showed both maximum percentage removal (40.49%) and amount ($2.02 \mu\text{g}/100 \text{ mL}^{-1}$) at the lowest tested concentration of 0.5 mgL^{-1} , indicating limited uptake at higher doses (Mallick & Rai, 1993).

For Zn^{2+} , Pb^{2+} , and Cr^{6+} , percentage removal decreased with increasing concentration, but the absolute removal amount peaked at intermediate levels ($1\text{--}3 \text{ mgL}^{-1}$), likely due to saturation of surface binding sites and reduced metabolic uptake at higher toxic loads (Jais et al., 2017; Mallick & Rai, 1993). Cd^{2+} uptake remained low at higher concentrations due to strong growth inhibition.

Cr^{6+} bioreduction

A distinctive feature of *C. minutissima* is its ability to enzymatically reduce Cr^{6+} to the less toxic Cr^{3+} . In our study, the highest bioreduction percentage (58%) occurred at 0.5 mgL^{-1} , while the maximum absolute amount reduced ($8.26 \mu\text{g}/\text{mL}^{-1}$) was at 3 mgL^{-1} . Our Cr^{6+} bioreduction (85.69%) was significantly higher ($p < 0.05$) than the 60–70% reported for *C. vulgaris* (June et al., 2010), demonstrating species-specific variation in detoxification capacity. This aligns with previous observations that Cr^{6+} bioreduction is primarily an intracellular process involving flavoprotein reductases (chromate reductases, nitroreductases) using nicotinamide adenine dinucleotide/ nicotinamide adenine dinucleotide phosphate (NADH/NADPH) or low molecular weight organics as electron donors (Lovley & Phillips, 1994; Cornelis et al., 2004; Cummings et al., 2007).

The high proportion of reduced chromium localized in the protoplasm supports the role of active enzymatic detoxification, which becomes less effective at higher Cr^{6+} concentrations due to metabolic inhibition (Saud et al., 2022). The bioreduction predominantly occurs within the protoplasm of the algal cells, indicating active intracellular enzymatic involvement. Key reductases, such as chromate reductases and nitroreductases, which are flavoproteins utilizing flavin mononucleotide (FMN) as a cofactor, mediate this transformation. These enzymes facilitate the transfer

of electrons from various cellular electron donors to Cr^{6+} , leading to its reduction. Common electron donors identified include:

- NADH and NADPH: These cofactors provide the necessary reducing equivalents for the enzymatic reduction of Cr^{6+} (Lovley & Phillips, 1994).
- Low molecular weight carbohydrates, amino acids, and fatty acids: These organic compounds can also serve as electron donors, supporting the Cr^{6+} reduction process (Lovley & Phillips, 1994).

The intracellular environment of *C. minutissima* supports the active bioabsorption of chromium species, thereby facilitating this enzymatic processing. This enzymatic reduction is a vital cellular defense mechanism against the oxidative stress induced by chromium exposure. The extended exposure times in studies, typically around 13 days, allow for greater intracellular processing of chromium compared to shorter incubation periods where surface adsorption might be more prominent (Owen et al., 2010). This highlights the importance of operational parameters like hydraulic retention time in maximizing bioreduction efficiency.

Implications for wastewater treatment and future work

The robust performance of *C. minutissima* in removing heavy metals and nutrients from wastewater streams has significant implications for industrial wastewater treatment (Yang et al., 2015; Rajalakshmi et al., 2021). The results suggest that *C. minutissima* cultures, particularly with an initial density exceeding 10^6 cells mL^{-1} , can serve as an effective bioremediation tool for industrial effluents containing low to moderate concentrations of heavy metals (Mallick & Rai, 1993). At optimal growth conditions, this species achieves impressive removal efficiencies: up to 98.63% for Zn^{2+} , 93.15% for Pb^{2+} , 85.69% for Cr^{6+} , and 40.49% for Cd^{2+} at 0.5 mgL^{-1} concentrations. For higher metal concentrations, proportionally higher initial algal densities are likely required to maintain high removal efficiency, a factor influenced by biomass productivity. The high removal efficiencies at low concentrations suggest that *C. minutissima* is particularly suited for tertiary treatment of effluents containing low-to-moderate heavy metal loads. Integration with existing treatment systems could allow simultaneous nutrient and metal removal while generating biomass for valorization into biofuels, biofertilizers, or nutraceuticals (Yang et al., 2015).

Operational challenges and scalability

While promising, the large-scale industrial application of algal bioremediation faces several operational challenges (Roberts et al., 2013).

- **Complex Wastewater Matrices:** Real industrial effluents often contain competing ions, varied organic matter, and fluctuating pH, which can influence metal bioavailability and algal uptake performance (Malla et al., 2015). Maintaining optimal growth conditions in such complex environments requires careful management and optimization (Cao et al., 2014).
- **Biomass Harvesting:** The separation of microalgal biomass from large volumes of water remains a significant economic and practical hurdle for full-scale implementation (Lavriničs & Juhna, 2017). Cost-effective harvesting methods are essential for wider adoption.
- **Scalability and Cost-effectiveness:** While pilot-scale photobioreactors have shown promise for nutrient removal and biomass production, scaling up these systems for industrial volumes presents challenges related to energy consumption and capital costs. Preventing contamination by other microbes is also a crucial aspect for large-scale operations (Min et al., 2011; Roberts et al., 2013).
- **Process Efficiency in Cold Climates:** The efficiency of algal bioremediation processes can be hampered in colder climates, necessitating further research into robust strains or system modifications (Lavriničs & Juhna, 2017).

Challenges remain in scaling up, especially biomass harvesting, maintaining monocultures in open systems, and coping with complex wastewater matrices (Malla et al., 2015; Lavriničs & Juhna, 2017).

Future prospects

Further pilot-scale testing using actual industrial effluents is crucial to validate the performance of *C. minutissima* under the complexities of real wastewater chemistries (Malla et al., 2015). Research needs include:

- **Strain Engineering:** Genetic and metabolic engineering can enhance *C. minutissima*'s metal tolerance, uptake specificity, and biotransformation capabilities (Mallick & Rai, 1993). This involves modifying cell surface

properties, improving transport proteins, and enhancing intracellular metal sequestration by over expressing metal-binding peptides like metallothioneins and phytochelatins.

- Reactor Design and System Integration: Optimization of photobioreactor designs, exploring algal immobilization techniques, and studying co-cultivation with bacteria can improve process robustness and overcome scalability constraints (Min et al., 2011; Singh et al., 2011).
- Advanced Monitoring and Modeling: Developing advanced tools for understanding metal speciation, sorption kinetics, and algal metabolic pathways in complex systems is essential.
- Regulatory Compliance: The ongoing discharge of toxic substances from industrial sectors necessitates effective heavy metal removal to comply with international guidelines and regulatory standards (Koju et al., 2022). Biological treatment technologies, including microalgae, are crucial for meeting these stringent limits.

Overall, *C. minutissima* represents a significant advancement in sustainable wastewater treatment, offering a multifaceted approach to address both heavy metal pollution and nutrient removal while simultaneously producing valuable biomass (Yang et al., 2015). Continued research and development in engineering and process optimization are vital to realize its full industrial potential.

Conclusion

This study demonstrates that *C. minutissima* can effectively remove low concentrations (0.5–10 mg L⁻¹) of Cd²⁺, Cr⁶⁺, Pb²⁺, and Zn²⁺ under optimized laboratory conditions. Removal efficiencies varied significantly among metals, with Zn²⁺ showing the highest removal percentage at low concentrations and Cd²⁺ exhibiting the strongest toxicity. Pb²⁺ showed higher absolute uptake amounts, while Zn²⁺ removal was most efficient at trace concentrations. Cr⁶⁺ was actively reduced to Cr³⁺ within algal cells, confirming intracellular detoxification. These results suggest that *C. minutissima* is a promising candidate for removing trace levels of heavy metals under controlled conditions. However, large-scale applicability remains to be validated. Future research should focus on experiments with real industrial wastewater, pilot-scale trials, and assessment of the fate of metal-laden biomass.

Acknowledgement

The authors gratefully acknowledge the All India Council for Technical Education (AICTE), New Delhi, for providing financial assistance in the form of a Ph.D. stipend. The authors also extend their sincere thanks to the Dr. B. R. Ambedkar National Institute of Technology (NIT), Jalandhar, for providing the laboratory facilities and research support necessary to carry out this work.

Author contributions

Shailendra Kumar Singh: Conceptualization and methodology; Ajay Bansal and M. K. Jha: Supervision; Gerard Abraham: Algae source; Rupak Kumar: Drafting and proof reading.

Conflict of interest

The authors declare no conflict of interest.

Ethics approval

Not applicable.

References

Ahmed, M., Mavukkandy, M. O., Giwa, A., Elektorowicz, M., Katsou, E., Khelifi, O., & Hasan, S. W. (2022). Recent developments in hazardous pollutants removal from wastewater and water reuse within a circular economy. *NPJ Clean Water*, 5(1), 12.

- Areco, M. M., Hanela, S., Duran, J., & Afonso, M. D. S. (2012). Biosorption of Cu(II), Zn(II), Cd(II) and Pb(II) by dead biomasses of green alga *Ulva lactuca* and the development of a sustainable matrix for adsorption implementation. *Journal of Hazardous Materials*, 213–214, 123–132. <https://doi.org/10.1016/j.jhazmat.2012.01.073>.
- ASTM. (2006). *Standard guide for conducting static toxicity tests with microalgae (E 1218-04)*. ASTM International.
- ASTM. (2010). *Standard Test Method for the Determination of Hexavalent Chromium in Workplace Air by Ion Chromatography and Spectrophotometric Measurement Using 1,5-diphenylcarbazide (ASTM D6832 - 08)*. American Society for Testing and Materials, United States.
- Bates, S. S., Tessier, A., Campbell, P. G. C., & Buffle, J. (1982). Zinc adsorption and transport by *Chlamydomonas variabilis* and *Scenedesmus subspicatus* (Chlorophyceae) grown in semi-continuous cultures. *Journal of Phycology*, 18(4), 521–529.
- Becker, E. W. (1994). *Microalgae: Biotechnology and microbiology*. Cambridge University Press.
- Bhatnagar, A., Bhatnagar, M., Chinnasamy, S., & Das, K. C. (2010). *Chlorella minutissima*—A promising fuel alga for cultivation in municipal wastewaters. *Applied Biochemistry and Biotechnology*, 161(1–8), 523–536.
- Cao, J., Yuan, H., Li, B., & Yang, J. (2014). Significance evaluation of the effects of environmental factors on the lipid accumulation of *Chlorella minutissima* UTEX 2341 under low-nutrition heterotrophic condition. *Bioresource Technology*, 152, 177–184.
- Chen, H., Chiang, R. H., & Storey, V. C. (2012). Business intelligence and analytics: From big data to big impact. *MIS quarterly*, 1165–1188.
- Cornelis, R., Caruso, J., Crews, H., & Heumann, K. G. (2004). *Handbook of elemental speciation: Techniques and methodology*. John Wiley & Sons.
- Cummings, D. E., Fendorf, S., Singh, N., Sani, R. K., Peyton, B. M., & Magnuson, T. S. (2007). Reduction of Cr(VI) under acidic conditions by the facultative Fe(III)-reducing bacterium *Acidiphilium cryptum*. *Environmental Science & Technology*, 41(1), 146–152.
- Danouche, M., El Ghatchouli, N., & Arroussi, H. (2022). Overview of the management of heavy metals toxicity by microalgae. *Journal of Applied Phycology*, 34(1), 475–488.
- Dao, T.-S., Le, N.-H.-S., Vo, M.-T., Vo, T.-M.-C., & Phan, T.-H. (2018). Growth and metal uptake capacity of microalgae under exposure to chromium. *Journal of Vietnamese Environment*, 9(1), 38–43.
- Dheri, G. S., Brar, M. S., & Malhi, S. S. (2007). Heavy-metal concentration of sewage-contaminated water and its impact on underground water, soil, and crop plants in alluvial soils of northwestern India. *Communications in Soil Science and Plant Analysis*, 38(9–10), 1353–1370.
- Eaton, A. D., Clesceri, L. S., Rice, E. W., & Greenberg, A. E. (Eds.). (2005). *Standard methods for the examination of water and wastewater* (21st ed.). American Public Health Association (APHA) Press. Washington, DC.
- Ge, Z., Zhang, H., Zhang, Y., Yan, C., & Zhao, Y. (2013). Purifying synthetic high-strength wastewater by microalgae *Chlorella vulgaris* under various light emitting diode wavelengths and intensities. *Journal of Environmental Health Science and Engineering*, 11(1), 8.
- Jais, N. M., Mohamed, R. M. S. R., Al-Gheethi, A. A., & Hashim, M. A. (2017). The dual roles of phycoremediation of wet market wastewater for nutrients and heavy metals removal and microalgae biomass production. *Clean Technologies and Environmental Policy*, 19(1), 37–52.
- Janssen, M. G. J. (2002). *Cultivation of microalgae: Effect of light/dark cycles on biomass yield* (Doctoral dissertation). Wageningen University, Netherlands.

- Jyoti, J., & Awasthi, M. (2014). Bioremediation of wastewater chromium through microalgae: a review. *Int J Eng Res*, 3, 1210-1215.
- Khurana, M. P. S., Nayyar, V. K., Bansal, R. L., & Singh, M. V. (2003). Heavy metal pollution in soils and plants through untreated sewage water. In V. P. Singh & R. N. Yadava (Eds.), *Ground water pollution, water and environment: Proceedings of the International Conference on Water and Environment (WE-2003), Dec. 15–18* (Vol. 1518, pp. 487–490). Allied Publishers Pvt. Ltd.
- Kinuthia, G. K., Ngure, V., Beti, D., Lugalia, R., Wangila, A., & Kamau, L. (2020). Levels of heavy metals in wastewater and soil samples from open drainage channels in Nairobi, Kenya: community health implication. *Scientific reports*, 10(1), 8434. <https://doi.org/10.1038/s41598-020-65359-5>.
- Koju, P., Shrestha, R., Shrestha, A., Tamrakar, S., Rai, A., Shrestha, P., ... & Shakya Shrestha, S. (2022). Antimicrobial resistance in *E. coli* isolated from chicken cecum samples and factors contributing to antimicrobial resistance in Nepal. *Tropical Medicine and Infectious Disease*, 7(9), 249.
- Lavrinovičs, A., & Juhna, T. (2017). Review on challenges and limitations for algae-based wastewater treatment. *Construction Science*, 20(1), 17–25.
- Lovley, D. R., & Phillips, E. J. P. (1994). Reduction of chromate by *Desulfovibrio vulgaris* and its c_3 cytochrome. *Applied and Environmental Microbiology*, 60(2), 726–728. <https://doi.org/10.1128/aem.60.2.726-728.1994>.
- Luo, C. L. (2003). The mechanisms of heavy metal uptake and accumulation in plants. *Chinese Bulletin of Botany*, 20(1), 59–64.
- Malakootian, M., Yousefi, Z., & Limoni, Z. K. (2019). Removal of lead from battery industry wastewater by *Chlorella vulgaris* as green micro-algae (Case study: Kerman, Iran). *Desalination and Water Treatment*, 141, 248–255.
- Malla, F. A., Khan, S. A., Sharma, G. K., Gupta, N., & Abraham, G. J. E. E. (2015). Phycoremediation potential of *Chlorella minutissima* on primary and tertiary treated wastewater for nutrient removal and biodiesel production. *Ecological Engineering*, 75, 343–349.
- Mallick, N., & Rai, L. C. (1993). Influence of culture density, pH, organic acids and divalent cations on the removal of nutrients and metals by immobilized *Anabaena doliolum* and *Chlorella vulgaris*. *World Journal of Microbiology and Biotechnology*, 9(2), 196–201.
- McKay, G., & Porter, J. F. (1997). Equilibrium parameters for the sorption of copper, cadmium and zinc ions onto peat. *Journal of Chemical Technology & Biotechnology*, 69(3), 309-320.
- Min, M., Wang, L., Li, Y., Mohr, M. J., Hu, B., Zhou, W., & Ruan, R. (2011). Cultivating *Chlorella* sp. in a pilot-scale photobioreactor using centrate wastewater for microalgae biomass production and wastewater nutrient removal. *Applied Biochemistry and Biotechnology*, 165(1), 123–137. <https://doi.org/10.1007/s12010-011-9238-7>.
- Monteiro, C. M., Castro, P. M. L., & Malcata, F. X. (2012). Metal uptake by microalgae: Underlying mechanisms and practical applications. *Biotechnology Progress*, 28(2), 299–311. <https://doi.org/10.1002/btpr.1504>.
- Novák, Z., Harangi, S., Baranyai, E., Gonda, S., Béres, V. B., & Bácsi, I. (2020). Effects of metal quantity and quality on the removal of zinc and copper by two common green microalgae (Chlorophyceae) species. *Phycological Research*, 68(3), 227–235.
- Olasehinde, T. A., Olaniran, A. O., & Okoh, A. I. (2019). Phenolic composition, antioxidant activity, anticholinesterase potential and modulatory effects of aqueous extracts of some seaweeds on β -amyloid aggregation and disaggregation. *Pharmaceutical Biology*, 57(1), 460–469.
- Owen, A. M., Hampshire, A., Grahn, J. A., Stenton, R., Dajani, S., Burns, A. S., ... & Ballard, C. G. (2010). Putting brain training to the test. *Nature*, 465(7299), 775-778.

- Perez-García, O., Escalante, F. M. E., de-Bashan, L. E., & Bashan, Y. (2011). Heterotrophic cultures of microalgae: Metabolism and potential products. *Water Research*, *45*(1), 11–36. <https://doi.org/10.1016/j.watres.2010.08.037>.
- Pérez-Rama, M., Alonso, J. A., López, C. H., & Vaamonde, E. (2002). Cadmium removal by living cells of marine microalga *Tetraselmis suecica*. *Bioresource Technology*, *84*(3), 265–270.
- Rajalakshmi, A. M., Silambarasan, T., & Dhandapani, R. (2021). Small-scale photobioreactor treatment of tannery wastewater, heavy metal biosorption and CO₂ sequestration using microalga *Chlorella* sp.: A biodegradation approach. *Applied Water Science*, *11*(7), 108.
- Rippka, R., Deruelles, J., Waterbury, J. B., Herdman, M., & Stanier, R. Y. (1979). Generic assignments, strain histories and properties of pure cultures of cyanobacteria. *Journal of General Microbiology*, *111*(1), 1–61. <https://doi.org/10.1099/00221287-111-1-1>.
- Roberts, D. A., de Nys, R., & Paul, N. A. (2013). The effect of CO₂ on algal growth in industrial wastewater for bioenergy and bioremediation applications. *PLoS One*, *8*(11), e81631. <https://doi.org/10.1371/journal.pone.0081631>.
- Salama, E. S., Roh, H. S., Dev, S., Khan, M. A., Abou-Shanab, R. A., Chang, S. W., & Jeon, B. H. (2019). Algae as a green technology for heavy metals removal from various wastewater. *World Journal of Microbiology and Biotechnology*, *35*(5), 75.
- Satoh, A., Vudikaria, L. Q., Kurano, N., & Miyachi, S. (2005). Evaluation of the sensitivity of marine microalgal strains to the heavy metals, Cu, As, Sb, Pb and Cd. *Environment International*, *31*(5), 713–722.
- Saud, S., Wang, D., Fahad, S., Javed, T., Jaremko, M., Abdelsalam, N. R., & Ghareeb, R. Y. (2022). The impact of chromium ion stress on plant growth, developmental physiology, and molecular regulation. *Frontiers in Plant Science*, *13*, 994785. <https://doi.org/10.3389/fpls.2022.994785>.
- Saxena, G., Kumar, L., Hariri, S. M., Roy, A., Kundu, K., & Bharadvaja, N. (2016). Identification of potential culture conditions for enhancing the biomass production of microalga *Chlorella minutissima*. *Expert Opinion on Environmental Biology*, *1*(2), 1–6.
- Shuler, M. L., & Kargi, F. (2002). *Bioprocess engineering: Basic concepts* (2nd ed.). Prentice Hall.
- Singh, S. K., Bansal, A., Jha, M. K., & Dey, A. (2011). Comparative studies on uptake of wastewater nutrients by immobilized cells of *Chlorella minutissima* and dairy waste isolated algae. *Indian Chemical Engineer*, *53*(4), 205–213.
- Singh, S. K., Bansal, A., Jha, M. K., & Dey, A. (2012). An integrated approach to remove Cr(VI) using immobilized *Chlorella minutissima* grown in nutrient rich sewage wastewater. *Bioresource Technology*, *104*, 257–265.
- Singh, S. K., Bansal, A., Jha, M. K., & Jain, R. (2013). Production of biodiesel from wastewater grown *Chlorella minutissima*. *Indian Journal of Chemical Technology*, *20*(5), 341–345.
- Spain, O., Plöhn, M., & Funk, C. (2021). The cell wall of green microalgae and its role in heavy metal removal. *Physiologia Plantarum*, *173*(2), 526–535.
- Sultana, N., Hossain, S. Z., Mohammed, M. E., Irfan, M. F., Haq, B., Faruque, M. O., ... & Hossain, M. M. (2020). Experimental study and parameters optimization of microalgae based heavy metals removal process using a hybrid response surface methodology-crow search algorithm. *Scientific Reports*, *10*(1), 15068. <https://doi.org/10.1038/s41598-020-72236-8>.
- Yang, J., Cao, J., Xing, G., & Yuan, H. (2015). Lipid production combined with biosorption and bioaccumulation of cadmium, copper, manganese and zinc by oleaginous microalgae *Chlorella minutissima* UTEX 2341. *Bioresource Technology*, *175*, 537–544.

Zhu, M., Nie, G., Meng, H., Xia, T., Nel, A., & Zhao, Y. (2013). Physicochemical properties determine nanomaterial cellular uptake, transport, and fate. *Accounts of Chemical Research*, 46(3), 622–631. <https://doi.org/10.1021/ar300031y>.